

Kinetics and Thermodynamics of Copper(I)/Dioxygen Interaction

KENNETH D. KARLIN,^{*,†} SUSAN KADERLI,[‡] AND ANDREAS D. ZUBERBÜHLER^{*,‡}

Department of Chemistry, The Johns Hopkins University, Baltimore, Maryland 21218, and Institute of Inorganic Chemistry, University of Basel, CH-4056 Basel, Switzerland

Received August 16, 1996

Introduction

In this Account, we summarize our recent research concerning the formation, stabilities, and structures of discrete copper–dioxygen complexes, arising from detailed variable temperature stopped-flow kinetic–spectroscopic studies on well-characterized synthetic copper coordination complexes. Low-molecular-weight copper(I) complex reactivity with dioxygen derives interest from the existence of facile Cu(I)/Cu(II) redox interconversion chemistry and ensuing involvement in stoichiometric or catalytic oxidation and oxygenation of organic substrates.¹ This work is also relevant to bioinorganic chemistry,^{2–5} since in nature a variety of copper proteins are essential constituents of aerobic organisms, including hemocyanins (arthropodal and molluscan O₂ carriers) and enzymes that “activate” O₂, promoting oxygen atom incorporation into biological substrates. The latter include tyrosinase (Tyr), dopamine β-monooxygenase (DβM), and the related peptidyl α-hydroxylating monooxygenase (PHM), as well as the bacterial membrane protein methane monooxygenase (*p*-MMO). “Blue” multicopper oxidases⁴ (e.g., laccase, ascorbate oxidases, and ceruloplasmin (CP)) promote substrate (e.g., amine, phenol) one-electron oxidations while reducing O₂ to water, and CP or related enzymes may be involved in copper (and coupled iron) metabolism.⁶ Cytochrome *c* and quinol oxidases transduce energy from the same 4e[−]/4H⁺ reduction of O₂ occurring

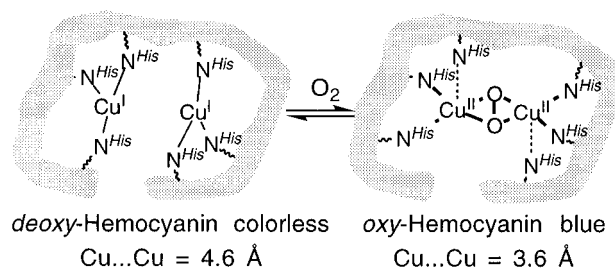
Kenneth D. Karlin received his B.S. degree from Stanford University (1970) and a Ph.D. in inorganic chemistry from Columbia University (1975), with Professor Stephen J. Lippard. After a postdoctoral in organometallic chemistry working with Professor (Lord) Jack Lewis at Cambridge, England, he joined the Chemistry Department at the State University of New York (SUNY) at Albany in 1977. In 1990, he moved as Professor to his present position at The Johns Hopkins University. His main interests have been in the design of ligands and coordination complexes for the structural, spectroscopic, and functional modeling of copper proteins which process O₂ or nitrogen oxide species.

Susan Kaderli completed her training in medical chemistry in 1984. As a permanent co-worker at the Institute, she has become an expert in kinetics and equilibrium studies and has been a key investigator in the work summarized in this Account. For many years she has been a leading figure of Swiss handball.

Andreas D. Zuberbühler received his diploma (1963) and his Ph.D. in inorganic chemistry (1965, with Professor Silvio Fallab) at the University of Basel, Switzerland. In his postdoctoral studies with Professor Howard S. Mason he became interested in bioinorganic chemistry. Back to Basel, he became Privatdozent in 1969 and Professor in 1978. His research interests have been in thermodynamics and reactivity of biomimetic transition metal complexes as well as in numerical methods of data reduction. He is a member of the federal commission for the safety of nuclear power plants and presently chairman of the energy commission of the Swiss Academy of Engineering Sciences.

at a heme–Cu binuclear center, and couple this to membrane proton translocation, utilized in ATP synthesis.⁵ Amine oxidases and galactose oxidase effect amine → aldehyde oxidative deaminations and alcohol → aldehyde oxidative dehydrogenations, respectively.^{1,3} Copper ion reactions with reduced dioxygen derivatives (e.g., superoxide (O₂[−]), hydrogen peroxide) are essential in Cu–Zn superoxide dismutase,⁷ and may be involved in copper-mediated oxidative damage in biological media, including possibly in Alzheimer’s disease.⁸

Direct interaction of O₂ with reduced (Cu(I)_{*n*}) enzymes is essential, but only for hemocyanin, tyrosinase, and recently laccase⁴ has direct experimental (spectroscopic) evidence bearing upon dioxygen adducts been available. A more detailed understanding and baseline appreciation of copper(I)/dioxygen interactions is desirable, since the diverse nature of the functions and active site composition of these copper enzymes ensures that varied Cu(I)_{*n*}/O₂ reactivity patterns and accompanying protonation–reduction chemistry exist. Both Hc and Tyr exhibit a Cu(I):O₂ = 2:1 reaction stoichiometry, with binding occurring in a side-on μ-η²:η²-bridging peroxo (O₂[−]) fashion, as indicated below:^{4,9}



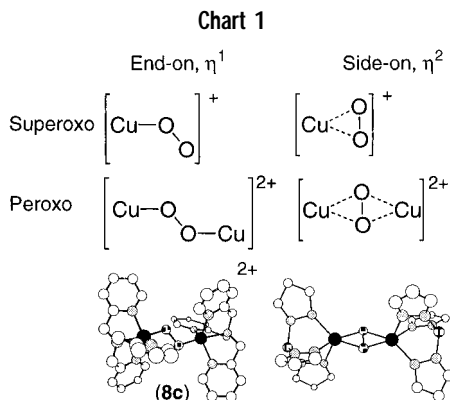
The difference is that the protected buried active site in Hc is instead accessible to phenolic substrates in Tyr.⁴ By contrast, biochemical evidence suggests that the O₂ and substrate oxygenation chemistry occurs at a single copper center in the monooxygenases DβM and PHM.³ A trinuclear copper active site cluster is suggested to mediate alkane hydroxylations in *p*-MMO, while X-ray structures have confirmed such Cu₃ centers in “blue” copper oxidases.⁴

In earlier work on chemical systems, unstable copper–dioxygen intermediates were commonly postulated, and kinetic evidence in a number of cases clearly implicated CuO₂⁺ and Cu₂O₂²⁺ species, but without any knowledge of their stabilities, spectroscopic properties, or structures.¹⁰ One piece of hard data concerning a fleeting species was

[†] The Johns Hopkins University.

[‡] University of Basel.

- (1) Kitajima, N.; Moro-oka, Y. *Chem. Rev.* **1994**, *94*, 737–757.
- (2) *Bioinorganic Chemistry of Copper*; Karlin, K. D., Tyeklár, Z., Eds.; Chapman & Hall: New York, 1993.
- (3) Klinman, J. P. *Chem. Rev.* **1996**, *96*, 2541–2561.
- (4) Solomon, E. I.; Sundaram, U. M.; Machonkin, T. E. *Chem. Rev.* **1996**, *96*, 2563–2605.
- (5) Ferguson-Miller, S.; Babcock, G. T. *Chem. Rev.* **1996**, *96*, 2889–2907.
- (6) Kaplan, J.; O’Halloran, T. V. *Science* **1996**, *271*, 1510–1512.
- (7) Fridovich, I. *Annu. Rev. Biochem.* **1995**, *64*, 97–112.
- (8) Multhaupt, G.; Schlicksupp, A.; Hesse, L.; Beher, D.; Ruppert, T.; Masters, C. L.; Beyreuther, K. *Science* **1996**, *271*, 1406–1409.
- (9) Magnus, K. A.; Hazes, B.; Ton-That, H.; Bonaventura, C.; Bonaventura, J.; Hol, W. G. J. *Proteins: Struct., Funct., Genet.* **1994**, *19*, 302–309.
- (10) Karlin, K. D.; Tyeklár, Z.; Zuberbühler, A. D. In *Bioinorganic Catalysis*; Reedijk, J., Ed.; Marcel Dekker, Inc.: New York, 1993; pp 261–315.



known, a bimolecular rate constant of formation ($9.5 \times 10^5 \text{ M}^{-1} \text{ s}^{-1}$) starting from $(\text{Cu}_{\text{aq}})^+$.¹⁰ The situation has changed dramatically in the last decade or so, as we and others have been able to stabilize and characterize synthetic copper–dioxygen adducts of a variety of types.^{1,2,10,11}

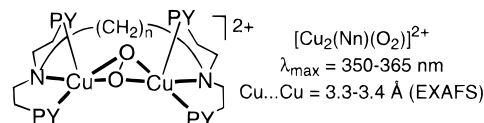
Four principal binding modes are established for the interaction of transition metal complexes with dioxygen (Chart 1), and all are suggested or proven for copper. These include end-on binding, as found in hemoglobin, and side-on binding, as in hemocyanin. Both may be combined with $\text{Cu(I)}/\text{O}_2 = 1:1$ (superoxo) and $\text{Cu(I)}/\text{O}_2 = 2:1$ (peroxo) stoichiometry, and three of the four types now have representative X-ray structures. The first such description for a copper–dioxygen adduct, synthetic or protein, came with our characterization of the 2:1 adduct $[(\text{TMPA})\text{Cu}^{\text{II}}]_2(\text{O}_2^{2-})^{2+}$ (**8c**) (Chart 1) (with PF_6^- or ClO_4^- counteranions), formed by reversible oxygenation of precursor complex $[(\text{TMPA})\text{Cu}^{\text{I}}(\text{RCN})]^+$ (**8a**) ($\text{R} = \text{Me}, \text{Et}$, $\text{TMPA} = \text{tris}(2\text{-pyridylmethyl})\text{amine}$).¹² Dication **8c** is best described as a peroxodicopper(II) species. It is essentially diamagnetic, possessing a *trans*- μ -1,2- $\text{Cu}_2\text{O}_2^{2+}$ moiety with $\text{Cu} \cdots \text{Cu} = 4.36 \text{ \AA}$ and $\text{O}-\text{O} = 1.432 \text{ \AA}$ (Chart 1). Other relevant physical properties are $\nu_{\text{O}-\text{O}} = 831 \text{ cm}^{-1}$ (resonance Raman),^{10–12} and UV–vis (i.e., peroxo-to-Cu(II) LMCT) bands at 440 nm (sh, $\epsilon = 2000 \text{ M}^{-1} \text{ cm}^{-1}$), $\lambda_{\text{max}} = 525 \text{ nm}$ (11 500) and $\sim 600 \text{ nm}$ (sh, ~ 7600), and a d–d band at 1035 nm (180). Kitajima and co-workers used a sterically hindered tridentate ligand in characterizing $\{\text{Cu}^{\text{II}}[\text{HB}(3,5\text{-}i\text{Pr}_2\text{pz})_3]\}_2(\text{O}_2^{2-})$ ($\text{HB}(3,5\text{-}i\text{Pr}_2\text{pz})_3 = \text{hydrotris}(3,5\text{-diisopropylpyrazolyl})\text{borate}$ anion), which has a side-on ligated $\mu\text{-}\eta^2\text{:}\eta^2\text{-peroxodicopper(II)}$ structure (Chart 1), with physical properties (i.e., $\text{Cu} \cdots \text{Cu} = 3.56 \text{ \AA}$, $\text{O}-\text{O} = 1.412 \text{ \AA}$, $\nu_{\text{O}-\text{O}} = 741 \text{ cm}^{-1}$ (resonance Raman), $\lambda_{\text{max}} = 349 \text{ nm}$ ($\epsilon = 21\,000 \text{ M}^{-1} \text{ cm}^{-1}$), 551 nm (790)) closely matching those of *Limulus polyphemus* oxyhemocyanin.¹⁴ This important contribution to synthetic modeling of metalloproteins in fact preceded confirmation of the protein Cu_2O_2 side-on structure. More recently,¹³ a side-on superoxocopper(II) complex has been generated and structurally characterized by the same group; $\text{Cu}^{\text{II}}(\text{O}_2^-)(\text{HB}(3\text{-}t\text{Bu-5-}i\text{Prpz})_3)$ has $\lambda_{\text{max}} = 352 \text{ nm}$ (2330), $\text{O}-\text{O} = 1.22 (3) \text{ \AA}$, and $\nu_{\text{O}-\text{O}} = 1111 \text{ cm}^{-1}$ (resonance Raman).

Complexes with the TMPA tripodal tetradentate ligand found in complexes **1** and analogues have provided us

with a plethora of kinetic–thermodynamic information and insight, as described below. A great deal of success has also been enjoyed by employment of the bis(2-pyrid-2-ylethyl)amine (PY2) tridentate ligand moiety for copper(I), and copper–dioxygen complexes with this moiety will be discussed first. A key advance in the understanding of these copper(I)/dioxygen reactions has been the elaboration of computer programs for the application of numerical integration methods, and factor analysis, to data obtained from variable temperature (173–298 K) diode-array spectrophotometric stopped-flow kinetics experiments (360–775 nm, i.e., complete spectrum every 2 ms). These methods^{14,15} have enabled deduction of multistep kinetic mechanisms, including determination of relevant kinetic and equilibrium constants and elucidation of complete UV–vis spectra of intermediates.

Side-on Binding in Binuclear Complexes with Bis(2-pyrid-2-ylethyl)amine (PY2) Units

It is now known that a variety of tridentate ligands with nitrogen donors give copper(I) complexes which bind O_2 to give a side-on $\mu\text{-}\eta^2\text{:}\eta^2\text{-bridging}$ peroxodicopper(II) product having the characteristic intense UV (345–365 nm) charge-transfer band.^{1,10,11,16–20} On the basis of low-temperature solution extended X-ray absorption fine structure spectroscopic (EXAFS) investigation,²¹ we first proposed this for binuclear complexes containing $-(\text{CH}_2)_n-$ ($n = 3\text{--}5$) linked PY2 chelates, i.e., ligand Nn (PY = 2-pyridyl). In fact, O_2 (and CO) react reversibly with $[\text{Cu}^{\text{I}}_2(\text{Nn})]^{2+}$, producing $[\text{Cu}_2(\text{Nn})(\text{O}_2)]^{2+}$ (or $[\text{Cu}_2(\text{Nn})-$



$(\text{CO})_2]^{2+}$).^{1,10,11} As mentioned, Kitajima and co-workers subsequently proved this structure (with planar $\text{Cu}_2\text{--O}_2$ core) for $\{\text{Cu}^{\text{II}}[\text{HB}(3,5\text{-}i\text{Pr}_2\text{pz})_3]\}_2(\text{O}_2^{2-})$, Chart 1.¹ Together, these findings preceded any suggestion or confirmation of the side-on bound peroxo moiety in oxyhemocyanin, illustrating the significance of the bioinorganic synthetic modeling approach.

Dioxygen Complexes and Hydroxylation with $[\text{Cu}^{\text{I}}_2(\text{R-XYL-H})]^{2+}$ (1**).** The first system we examined by kinetics involved O_2 reaction with $[\text{Cu}^{\text{I}}_2(\text{R-XYL-H})]^{2+}$ (**1**, $\text{R} = \text{H}$), which results in hydroxylation of the 2-position of the arene (*m*-xylyl) spacer, leading to $[\text{Cu}^{\text{II}}_2(\text{R-XYL-O}^-)-$

(11) Karlin, K. D.; Tyeklár, Z. *Adv. Inorg. Biochem.* **1994**, *9*, 123–172.

(12) Tyeklár, Z.; Jacobson, R. R.; Wei, N.; Murthy, N. N.; Zubieta, J.; Karlin, K. D. *J. Am. Chem. Soc.* **1993**, *115*, 2677–2689.

(13) Fujisawa, K.; Tanaka, M.; Moro-oka, Y.; Kitajima, N. *J. Am. Chem. Soc.* **1994**, *116*, 12079–12080.

(14) Karlin, K. D.; Nasir, M. S.; Cohen, B. I.; Cruse, R. W.; Kaderli, S.; Zuberbühler, A. D. *J. Am. Chem. Soc.* **1994**, *116*, 1324–1336.

(15) Karlin, K. D.; Wei, N.; Jung, B.; Kaderli, S.; Niklaus, P.; Zuberbühler, A. D. *J. Am. Chem. Soc.* **1993**, *115*, 9506–9514.

(16) Sanyal, I.; Mahroof-Tahir, M.; Nasir, S.; Ghosh, P.; Cohen, B. I.; Gultneh, Y.; Cruse, R.; Farooq, A.; Karlin, K. D.; Liu, S.; Zubieta, J. *Inorg. Chem.* **1992**, *31*, 4322–4332.

(17) Mahapatra, S.; Halfen, J. A.; Wilkinson, E. C.; Que Jr., L.; Tolman, W. B. *J. Am. Chem. Soc.* **1994**, *116*, 9785–9786.

(18) Lynch, W. E.; Kurtz, D. M., Jr.; Wang, S.; Scott, R. A. *J. Am. Chem. Soc.* **1994**, *116*, 11030–11038.

(19) Sorrell, T. N.; Allen, W. E.; White, P. S. *Inorg. Chem.* **1995**, *34*, 952–960.

(20) Halfen, J. A.; Mahapatra, S.; Wilkinson, E. C.; Kaderli, S.; Young Jr., V. G.; Que Jr., L.; Zuberbühler, A. D.; Tolman, W. B. *Science* **1996**, *271*, 1397–1400.

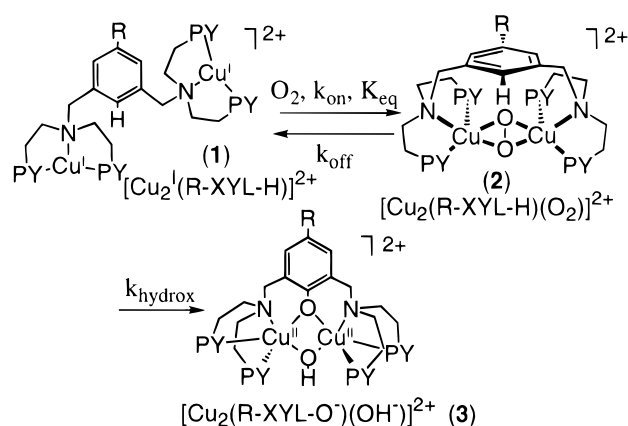
(21) Blackburn, N. J.; Strange, R. W.; Farooq, A.; Haka, M. S.; Karlin, K. D. *J. Am. Chem. Soc.* **1988**, *110*, 4263–4272.

Table 1. Kinetic–Thermodynamic Parameters for O₂ Reaction with [Cu^I₂(R-XYL-H)]²⁺ (1) and [Cu^{II}₂(XYL-O⁻)]⁺ (4)^a

R or ligand		NO ₂	H	C(CH ₃) ₃	F	H-XYL-O-
k_{on} (M ⁻¹ s ⁻¹)	183 K	110	410	470	7.2	>10 ⁶ ^b
	223 K	280	1300	1700	270	b
	$\Delta H_{\text{on}}^{\ddagger}$	6.4 ± 0.1	8.2 ± 0.1	9.1 ± 0.3	29 ± 1	b
k_{off} (s ⁻¹)	183 K	2.1 × 10 ⁻⁵	1.6 × 10 ⁻⁵	4.3 × 10 ⁻⁶	1.5 × 10 ⁻⁶	b
	223 K	0.027	0.076	0.094	0.025	b
	$\Delta H_{\text{off}}^{\ddagger}$	-167 ± 1	-146 ± 1	-140 ± 1	-66 ± 1	b
k_{hydrox} (s ⁻¹)	183 K	1.6 × 10 ⁻⁵	3.0 × 10 ⁻⁴	6.3 × 10 ⁻³	1.5 × 10 ⁻³	c
	223 K	0.013	0.13	0.96	0.18	c
	$\Delta H_{\text{hydrox}}^{\ddagger}$	55 ± 1	50 ± 1	41 ± 2	39 ± 1	c
K_{eq} (M ⁻¹)	183 K	6.7 × 10 ⁶	2.9 × 10 ⁷	1.2 × 10 ⁸	5.0 × 10 ⁶	6.5 × 10 ⁸
	223 K	1.3 × 10 ⁴	1.9 × 10 ⁴	1.9 × 10 ⁴	1.1 × 10 ⁴	2.7 × 10 ⁵
	$\Delta H_{\text{on}}^{\circ}$	-53 ± 1	-62 ± 1	-74 ± 4	-52 ± 3	-66 ± 1
	$\Delta S_{\text{on}}^{\circ}$	-159 ± 4	-196 ± 6	-250 ± 20	-156 ± 10	-192 ± 2
	$\Delta S_{\text{hydrox}}^{\ddagger}$	-32 ± 2	-35 ± 2	-59 ± 8	-82 ± 6	c

^a ΔH , kJ mol⁻¹; ΔS , J K⁻¹ mol⁻¹; all concentrations in mol dm⁻³. ^b Equilibration with O₂ in less than 5 ms at 178 K. ^c No oxygenation possible.

Scheme 1



(OH⁻)]²⁺ (3).¹⁴ This system has been proposed as a model for tyrosinase and represents one of very few examples in the literature wherein dioxygen can be employed to effect a hydrocarbon oxygenation, under extremely mild conditions, i.e., <1 atm of O₂ pressure and at room temperature or below. Other kinds of dicopper(I)/O₂ xylyl hydroxylations have subsequently been observed.^{1,10,11,22} The detailed proposed mechanism involves formation of a Cu₂-O₂ adduct by reaction of 1 with O₂, followed by electrophilic attack of this side-on bound peroxo moiety, present in favorable proximity to the π -system of the arene substrate.^{10,23} Low-temperature kinetic–spectroscopic studies^{14,24} carried out on oxygenation of derivatives [Cu₂^I(R-XYL-H)]²⁺ (1, R = NO₂, H, C(CH₃)₃, F) confirmed the presence of Cu₂-O₂ intermediates [Cu₂(R-XYL-H)(O₂)]²⁺ (2); the subsequent first-order irreversible step (k_{hydrox}) describes the oxygen atom insertion, producing [Cu^{II}₂(R-XYL-O⁻)(OH)]²⁺ (3) (Scheme 1), from which free phenol R-XYL-OH can be isolated. Here, we emphasize the initial process of reversible O₂ binding.

The reaction in dichloromethane was tracked between 171 and 299 K, following the 435 nm absorption, a band which is also characteristic of these [Cu₂(Nn)(O₂)]²⁺ type

complexes with side-on peroxo coordination, vide supra.²⁵ [Cu₂^I(R-XYL-H)]²⁺ (1, R = CN, OMe) also were synthesized and cleanly hydroxylate to give corresponding products [Cu^{II}₂(R-XYL-O⁻)(OH)]²⁺ (3). But these could not be studied by kinetics, as the cyano compound undergoes a strongly interfering photochemical process, while the methoxy analogue neither forms an O₂ adduct nor hydroxylates at low temperatures. Explanation for the latter phenomenon has been put forward.¹⁴

As can be seen from the data in Table 1, binding of O₂ (k_{on}) to these binuclear complexes is characterized by very low activation enthalpies of less than 10 kJ mol⁻¹. However, compensation occurs by extremely unfavorable activation entropies of -140 to -170 J K⁻¹ mol⁻¹. As a net result all complexes display rather similar k_{on} values at 223 K. The somewhat larger activation enthalpy of 29 kJ mol⁻¹ for the fluoro compound is explained by freezing out a complex conformation which is unfit for O₂ binding at low temperature, as indicated by low-temperature NMR. Trends observed in $\Delta H_{\text{off}}^{\ddagger}$ for release of O₂ from [Cu₂(R-XYL-H)(O₂)]²⁺ (2) (i.e., k_{off}) suggest that electron donating groups on the xylyl ring increase the copper–dioxygen bonding strength in these adducts.

Equilibrium parameters support this contention, as $\Delta H_{\text{on}}^{\circ}$ values correlate directly with xylyl substituent (R) inductive effects. For binuclear Cu₂-O₂ formation, all of the derivatives are characterized by large negative standard enthalpies and entropies. Also as seen for all copper–dioxygen complexes, and O₂ adducts with other metals,^{26,27} increasing favorable (negative) enthalpies are compensated by more negative entropies. In other words, when O₂ adduct formation leads to tighter metal–oxygen binding, this process leads to a species with fewer degrees of freedom.

We believe that the dicopper bound electrophilic μ - η^2 : η^2 -peroxo group in [Cu₂(R-XYL-H)(O₂)]²⁺ (2) is in very close proximity to the xylyl π -system, and this could

(22) Ghosh, D.; Lal, T. K.; Ghosh, S.; Mukherjee, R. *Chem. Commun.* **1996**, 13–14.

(23) Nasir, M. S.; Cohen, B. I.; Karlin, K. D. *J. Am. Chem. Soc.* **1992**, *114*, 2482–2494.

(24) Cruse, R. W.; Kaderli, S.; Karlin, K. D.; Zuberbühler, A. D. *J. Am. Chem. Soc.* **1988**, *110*, 6882–6883.

(25) Using 1,4,7-trialkyl-1,4,7-triazacyclononane ligands, Tolman and colleagues²⁰ recently showed that a visible absorption in this region can be indicative of a bis(μ -oxo)dicopper(III) species forming in rapid equilibrium with an isomeric μ - η^2 : η^2 -peroxodicopper(II) product of the LCu(I)-O₂ reaction.

(26) Niederhoffer, E. C.; Timmons, J. H.; Martell, A. E. *Chem. Rev.* **1984**, *84*, 137.

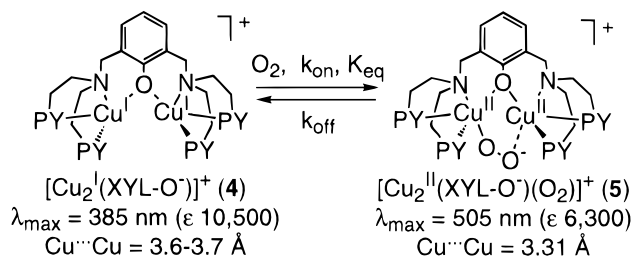
(27) Fallab, S.; Mitchell, P. R. *Adv. Inorg. Bioinorg. Mech.* **1984**, *3*, 311–377.

provide an explanation for the R group influence upon O₂ binding to [Cu₂(R-XYL-H)]²⁺ (**1**) and release. An alternative explanation is based on the nature of the O₂ binding process as described by *k*_{on} and *k*_{off} (Scheme 1) which are composed of at least three steps: (i) binding of O₂ to a single Cu (steady-state intermediate), (ii) preparation of a conformation of this {Cu...Cu-O₂} intermediate which is suitable for ring-closure, and (iii) formation of [Cu₂(R-XYL-H)(O₂)]²⁺ (**2**). The small Δ*H*_{on}[‡] values are in accord with a rapid preequilibrium in forming the intermediate, with the ring-closure process primarily determining the rates of formation and stabilities of **2**. The observed trends in substituent R for *k*_{off} (Scheme 1), for example, may not so much reflect actual O₂ binding strength in [Cu₂(R-XYL-H)(O₂)]²⁺ (**2**), but rather could be due to differences of conformation stabilities in the precursor {Cu...Cu-O₂} intermediates.

The hydroxylation step occurs with the absence of an observable isotope effect (i.e., H-XYL-D vs H-XYL-H),²⁴ while *k*_{hydrox} and Δ*H*_{hydrox}[‡] (Table 1) generally increase with electron-donating ability of R.¹⁴ Additional evidence for an electrophilic peroxide and electrophilic attack is presented elsewhere.^{10,23}

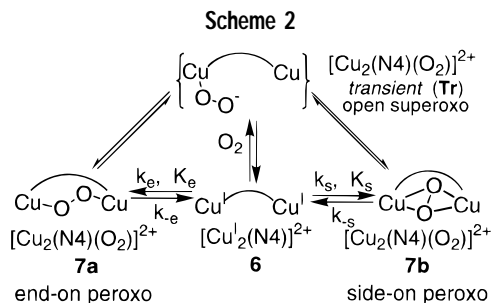
Dioxygen Binding in a Bridged Dicopper(I) Complex.

Dicopper(I) complex [Cu₂^I(XYL-O⁻)]⁺ (**4**) was the first complex we showed to reversibly bind O₂ (and CO) at low temperatures in dichloromethane.^{1,10,11} The product O₂ adduct is best described as a peroxodicopper(II) complex, [Cu₂^{II}(XYL-O⁻)(O₂²⁻)]⁺ (**5**), with ν_{O-O} = 803 cm⁻¹ (Raman).



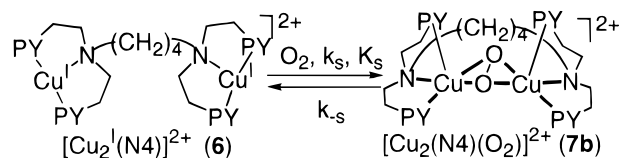
A detailed electronic spectroscopic analysis indicates only two charge-transfer transitions (505, 610 (sh) nm), sharply contrasting with that seen for a side-on bridging peroxodicopper(II) moiety, and consistent with unsymmetrical end-on peroxo coordination.

A stopped-flow kinetics study²⁴ revealed that the reaction of [Cu₂^I(XYL-O⁻)]⁺ (**4**) with dioxygen was too fast to be measured even at 173 K, and a lower limit for the oxygenation rate was determined to be *k*_{on} > 10⁶ M⁻¹ s⁻¹ (at 173 K). Thus, the bridging phenoxo group has the effect of preorganizing the dicopper(I) complex (lower activation barrier), leading to a rate of oxygenation of **4** which is more than 10 000 times faster than observed for the related complexes [Cu₂^I(R-XYL-H)]²⁺ (**1**), discussed above. Analysis of temperature dependent spectral changes yielded thermodynamic data for formation of this Cu:O₂ = 2:1 adduct [Cu₂^{II}(XYL-O⁻)(O₂²⁻)]⁺ (**5**): Δ*H*_{on}[°] = -66 kJ mol⁻¹, Δ*S*_{on}[°] = -192 J K⁻¹ mol⁻¹, *K*_{eq} = 7.6 × 10⁷ (193 K), *K*_{eq} = 58 (293 K). In fact, these values are within the range of thermodynamic parameters seen for formation of [Cu₂(R-XYL-H)(O₂)]²⁺ (**2**), Table 1. As a general conclusion, *the stability of dioxygen binding is driven by favorable enthalpies, but unfavorable reaction entropies preclude*



observation of Cu₂-O₂ (and Cu-O₂, *vide infra*) at room temperature.

Relative Stabilities of End-on and Side-on O₂ Binding, Both Observable in [Cu₂(N4)(O₂)]²⁺. The coordination sphere in the binuclear complex [Cu₂^I(N4)]²⁺ (**6**) is essentially the same as that found in [Cu₂^I(R-XYL-H)]²⁺ (**1**). However, with a presumably more flexible aliphatic -(CH₂)₄- linker and absence of an obvious position for electrophilic attack within [Cu₂(N4)(O₂)]²⁺ (**7b**, λ_{max} = 360



nm (ε ≈ 16 000), Cu...Cu = 3.4 Å (EXAFS)),^{21,28} **6** might be expected to react with O₂ more rapidly and be more stable than [Cu₂^I(R-XYL-H)]²⁺ (**1**). In fact, kinetic studies²⁸ on this seemingly simple system disclose a more complicated situation, where two different peroxo complexes form via a postulated open chain superoxo species, Scheme 2.

The kinetics allow elucidation of parameters (Table 2) for formation of either **7a** or **7b** from **6**; the detailed analysis²⁸ rules out sequential formation of the end-on (**7a**) species followed by side-on (**7b**) final product. In line with observations for [Cu₂^I(R-XYL-H)]²⁺ (**1**) (*vide supra*) and studies with a mononuclear copper(I) complex analogue with bis(2-pyrid-2-ylethyl)methylamine, the “open superoxo” transient species [Cu₂(N4)(O₂)]²⁺ (**Tr**) merely exists as a steady-state species and is invoked to avoid the necessity of synchronous binding of two copper ions to O₂ upon formation of the peroxo complexes. The negligible activation enthalpy of formation of intermediate **7a** is consistent with the proposed rapid preequilibrium involving **Tr**, rather than with an elementary process, **6** ↔ **7a**.

The thermodynamically more stable product [Cu₂(N4)(O₂)]²⁺ (**7b**) is assigned the μ-η²:η² side-on peroxo coordination by analogy to [Cu₂(R-XYL-H)(O₂)]²⁺ (**2**, λ_{max} = 440 nm). Also, the thermodynamic parameters (Δ*H*[°], Δ*S*[°]) are closely related to those of **2** (R = H), Tables 1 and 2. On the basis of spectral characteristics for intermediate **7a** (λ_{max} = 525 nm, shoulder near 600), this thermodynamically less stable species is assigned a μ-η¹:η¹ (end-on) Cu(II)-O-O-Cu(II) peroxo coordination, related to that established by X-ray for [{(TMPA)Cu^{II}]₂(O₂²⁻)]²⁺ (**8c**) (Chart 1). Open superoxo transient **Tr** is also suggested to have

(28) Jung, B.; Karlin, K. D.; Zuberbühler, A. D. *J. Am. Chem. Soc.* **1996**, *118*, 3763–3764.

Table 2. Kinetic–Thermodynamic Parameters for O₂ Reaction with [Cu₂(N4)]²⁺ (6)

	[Cu ₂ (N4)(O ₂)] ²⁺ (7a) end-on peroxo (λ _{max} = 525 nm)	[Cu ₂ (N4)(O ₂)] ²⁺ (7b) side-on peroxo (λ _{max} = 456 nm)
<i>k</i> (M ⁻¹ s ⁻¹)	183 K 223 K Δ <i>H</i> [‡] (kJ mol ⁻¹) Δ <i>S</i> [‡] (J K ⁻¹ mol ⁻¹)	<i>k</i> _e = 1.1 × 10 ⁴ <i>k</i> _e = 1.4 × 10 ⁴ 0 ± 3 -162 ± 18
<i>K</i> _{eq} (M ⁻¹)	183 K 223 K Δ <i>H</i> [‡] (kJ mol ⁻¹) Δ <i>S</i> [‡] (J K ⁻¹ mol ⁻¹)	<i>K</i> _e = (4.5 ± 0.4) × 10 ² <i>K</i> _e = 18 ± 8 -28 ± 3 -101 ± 19
		<i>k</i> _s = 9 × 10 ³ <i>k</i> _s = 8 × 10 ⁴ 18 ± 3 -70 ± 9
		<i>K</i> _s = 7 × 10 ⁷ <i>K</i> _s = 8 × 10 ⁵ -58 ± 2 -165 ± 8

an end-on Cu(II)–O–O⁻ ligation; if it were to have a side-on η² structure, attack of a second Cu(I) ion within **Tr** should lead directly to side-on product **7b**, and not the actually observed initial adduct **7a**. Intermediate **7a** is formed more quickly than is **7b** (Table 2), both significantly faster than [Cu^I(R-XYL-H)(O₂)]²⁺ (**2**) (*k* = 4.1 × 10² M⁻¹ s⁻¹); thus ligand flexibility (i.e., alkyl chain vs *m*-xylyl linker) indeed affords a more rapid O₂ reaction. The significantly more stable side-on species **7b** (*K*_{eq} = 7 × 10⁷ vs 4.5 × 10² M⁻¹ for **7a** at 183 K) has more than double the enthalpic stabilization (-58 vs -28 kJ mol⁻¹ for **7a**), likely derived from its pentacoordinate Cu(II) ions (each with two Cu–O_{peroxo} bonds), compared to the situation in intermediate **7a**, with assumed tetracoordination.²⁸

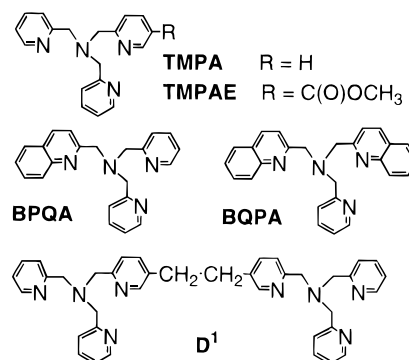
The N4 system has thus revealed two kinds of Cu₂–O₂ structures formed in the same system. The μ-η²:η²-peroxo complex is thermodynamically stable compared to the end-on species, and we have provided the first quantitative estimate of their relative stabilities. These results may pertain to multisubunit hemocyanin O₂ carriers, which exhibit highly cooperative O₂ binding behavior. With Cu⋯Cu = 4.6 Å in deoxy-Hc, O₂ reaction may initially lead to an end-on coordinated transient Cu–O₂ and Cu₂–O₂ species. Our work suggests that subsequent rearrangement to the observed μ-η²:η²-peroxodicopper(II) oxy-Hc product (Cu⋯Cu ≈ 3.6 Å) is thermodynamically driven. This must involve movement of copper ions and protein histidine ligands, exactly what has been proposed⁹ as the basis for induction of hemocyanin subunit–subunit cooperative binding interactions.

Terminal (End-on) O₂ Coordination in Complexes with Tetradentate Tripodal Ligands

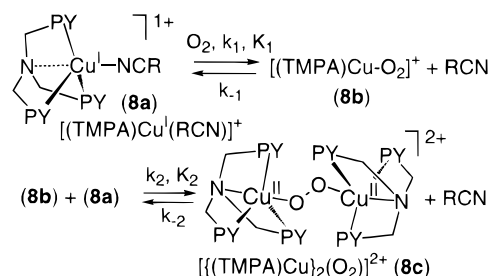
Mononuclear Complexes. As mentioned in the Introduction, the copper(I) complex of the ligand TMPA afforded [(TMPA)Cu^I]₂(O₂²⁻)²⁺ (**8c**), Chart 1. Having this structurally characterized copper–dioxygen product has provided a unique opportunity for study. Indeed, utilization of TMPA, quinolyl-substituted analogues, and a binucleating analogue, D¹ (Chart 2), leads to pseudoreversible O₂ binding by their copper(I) complexes, for which kinetic-thermodynamic analyses have been completed.^{15,29} TMPA represents the first case for which stepwise binding of O₂ to one and subsequently two copper moieties could be directly studied spectroscopically as well as kinetically. The mechanism (Scheme 3; PY = 2-pyridyl) applies also to TMPAE, BPQA, and BQPA; kinetic and thermodynamic parameters are collected in Table 3.

(29) Lee, D.-H.; Wei, N.; Murthy, N. N.; Tyeklár, Z.; Karlin, K. D.; Kaderli, S.; Jung, B.; Zuberbühler, A. D. *J. Am. Chem. Soc.* **1995**, *117*, 12498–12513.

Chart 2



Scheme 3



Cu:O₂ = 1:1 Superoxocopper(II) Complexes. As the primary products of reaction, Cu:O₂ = 1:1 adducts, i.e., superoxocopper(II) complexes, are of fundamental importance. Their subsequent reactivity (e.g., reduction, protonation, further metalation, substrate interaction) is clearly critical in oxidative processes, most prominently in monocopper protein centers (see the Introduction).

[(TMPA)Cu^I(RCN)]⁺ (**8a**) reacts with O₂, forming [(TMPA)Cu^{II}(O₂⁻)]⁺ (**8b**) as a transient intermediate, on the way to the ultimate μ-peroxo product [(TMPA)Cu^{II}]₂(O₂²⁻)²⁺ (**8c**) (Scheme 3 and Chart 1). TMPAE gives a strictly analogous behavior. By contrast, the bisquinolyl derivative BQPA preferentially forms a 1:1 adduct, [(BQPA)Cu(O₂)]⁺, with only ~10% of the 2:1 complex [(BQPA)Cu]₂(O₂)²⁺ (λ_{max} = 545 nm (ε = 5500))

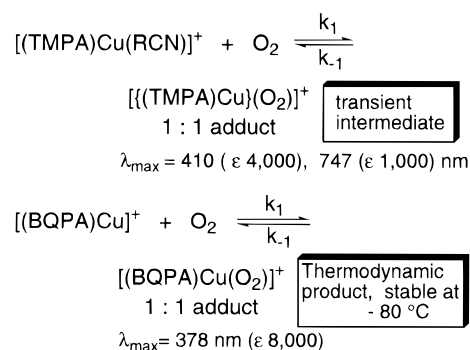


Table 3. Kinetic–Thermodynamic Parameters for O₂ Binding Tripod-Ligand–Copper(I) Complexes [(L)Cu]⁺

		[Cu(TMPA)] ⁺	[Cu(TMPAE)] ⁺	[Cu(BPQA)] ⁺	[Cu(BQPA)] ⁺	D ¹ complex
Kinetic Parameters						
k_1 (M ⁻¹ s ⁻¹)	183 K	2 × 10 ⁴	8.2 × 10 ³	<i>b</i>	18	1.6 × 10 ⁴
	298 K	8 × 10 ⁷	4 × 10 ⁷	<i>b</i>	6 × 10 ⁴	4 × 10 ⁶
	ΔH_1^\ddagger	32 ± 4	31 ± 5	<i>b</i>	30 ± 2	20 ± 1
	ΔS_1^\ddagger	14 ± 18	5 ± 29	<i>b</i>	-53 ± 8	-53 ± 6
k_{-1} (s ⁻¹)	183 K	8	29	<i>b</i>	6 × 10 ⁻³	8.0 ± 0.2
	298 K	2 × 10 ⁸	4 × 10 ⁸	<i>b</i>	2 × 10 ⁵	1.4 × 10 ⁷
	ΔH_{-1}^\ddagger	66 ± 4	63 ± 5	<i>b</i>	65 ± 4	55 ± 1
	ΔS_{-1}^\ddagger	137 ± 18	132 ± 29	<i>b</i>	72 ± 19	76 ± 6
k_2 (M ⁻¹ s ⁻¹)	183 K	3 × 10 ⁴	1.52 × 10 ⁴	<i>b</i>	<i>c</i>	35 ± 1
	298 K	1.8 × 10 ⁶	5.8 × 10 ⁶	<i>b</i>	<i>c</i>	6.8 × 10 ⁵
	ΔH_2^\ddagger	14 ± 1	21 ± 1	<i>b</i>	<i>c</i>	37 ± 1
	ΔS_2^\ddagger	-78 ± 2	-43 ± 3	<i>b</i>	<i>c</i>	-9 ± 2
k_{-2} (s ⁻¹)	183 K	1.5 × 10 ⁻⁴	2.1 × 10 ⁻⁵	1.9 × 10 ⁻⁴	<i>c</i>	0.39 ± 0.03
	298 K	1.2 × 10 ³	7 × 10 ²	1.6 × 10 ³	<i>c</i>	6.7 × 10 ³
	ΔH_{-2}^\ddagger	61 ± 3	66 ± 1	61 ± 1	<i>c</i>	37 ± 1
	ΔS_{-2}^\ddagger	19 ± 10	33 ± 5	21 ± 4	<i>c</i>	-49 ± 3
k_{on} (M ⁻² s ⁻¹) = $k_1 k_2 / k_{-1}$	183 K	6 × 10 ⁷	4.3 × 10 ⁶	3 × 10 ⁶	<i>c</i>	7.1 × 10 ⁴
	298 K	6 × 10 ⁵	5.2 × 10 ⁵	7 × 10 ⁵	<i>c</i>	1.8 × 10 ⁵
	$\Delta H_{\text{on}}^\ddagger$	-20 ± 2	-10.3 ± 0.2	-8 ± 1	<i>c</i>	1.7 ± 0.6
	$\Delta S_{\text{on}}^\ddagger$	-201 ± 5	-170 ± 1	-160 ± 2	<i>c</i>	-139 ± 3
Thermodynamic Parameters						
K_1 (M ⁻¹)	183 K	1.9 × 10 ³	2.8 × 10 ²	<i>d</i>	2.9 × 10 ³	2 × 10 ³
	298 K	0.34	9 × 10 ⁻²	<i>d</i>	0.4	0.27
	ΔH_1°	-34 ± 1	-32 ± 1	<i>d</i>	-35 ± 6	-35 ± 1
	ΔS_1°	-123 ± 4	-127 ± 3	<i>d</i>	-125 ± 27	-129 ± 2
K_2 (M ⁻¹)	183 K	2.2 × 10 ⁸	7 × 10 ⁸	<i>d</i>	2.0 × 10 ³	90
	298 K	1.5 × 10 ³	8 × 10 ³	<i>d</i>	40	100
	ΔH_2°	-47 ± 3	-45 ± 1	<i>d</i>	-15	0.5 ± 0.6
	ΔS_2°	-97 ± 10	-76 ± 6	<i>d</i>	-20	40 ± 3
$\beta_2 = K_1 K_2$	183 K	4.3 × 10 ¹¹	2.1 × 10 ¹¹	1.7 × 10 ¹⁰	6 × 10 ⁶	1.8 × 10 ⁵
	298 K	5 × 10 ²	7 × 10 ²	4.4 × 10 ²	20	27
	$\Delta H_{\text{on}}^\circ$	-81 ± 3	-77 ± 1	-69 ± 2	-50	-35 ± 1
	$\Delta S_{\text{on}}^\circ$	-220 ± 11	-203 ± 5	-181 ± 5	-145	-89 ± 2

^a ΔH , kJ mol⁻¹; ΔS , J K⁻¹ mol⁻¹. ^b Superoxo complex not observed with [Cu(BPQA)]⁺. ^c Only thermodynamic parameters obtained. ^d Not observed.

formed at -80 °C; benchtop (-80 °C) spectrophotometric monitoring and manometric O₂ uptake experiments confirm the Cu:O₂ = 1:1 stoichiometry, yielding the Cu(II)–(O₂⁻) complex. In fact, there is an “overshoot” in the initial O₂ reaction with [(BQPA)Cu]⁺, and as long as free copper(I) complex is present, the μ -peroxo binuclear species forms extremely rapidly, before it eventually converts to the more thermodynamically stable mononuclear [(BQPA)Cu(O₂)]⁺. Only equilibrium but not kinetic parameters could be obtained for formation of [(BQPA)Cu]₂(O₂)²⁺ (Table 3). For BPQA, a superoxo complex, [(BPQA)Cu(O₂)]⁺, could not be detected.

There are remarkable similarities in the kinetics and especially the thermodynamics for Cu:O₂ = 1:1 binding for these tetradentate ligand complexes (Table 3). Directly measured association rate constants (k_1) for TMPA and TMPAE are essentially identical, ~10⁴ M⁻¹ s⁻¹ at 183 K. These are accompanied by significant activation enthalpies (30–32 kJ mol⁻¹, including that observed for BQPA), which are much larger than those seen in general for formation of [Cu₂(R-XYL-H)(O₂)²⁺ (**2**) (i.e., <10 kJ mol⁻¹; Table 1). Even larger values are seen for Cu–O splitting, i.e., O₂ dissociation (k_{-1} ; 63–66 kJ mol⁻¹) for TMPA, TMPAE, and BQPA. The considerably smaller O₂ binding rate constants (k_1) observed for BQPA are exclusively due to a less favorable activation entropy, and we postulate that quinoyl group steric hindrance inhibits the rate of O₂ binding to [(BQPA)Cu(O₂)]⁺. Yet, a corresponding less favorable activation entropy for dissociation of O₂ in this latter BQPA complex renders overall superoxocopper(II)

[(L)Cu(O₂)]⁺ equilibrium parameters to be comparable: $\Delta H_1^\circ = -32$ to -35 kJ mol⁻¹ and $\Delta S_1^\circ = -123$ to -129 J K⁻¹ mol⁻¹ for TMPA, TMPAE, and BQPA. Redox potential differences (~200 mV) show that oxidation of Cu(I) to Cu(II) is favored with the TMPA compared to BQPA ligand, but this appears not to correlate too much with the stability of the LCu(II)–(O₂⁻) product. Further systematic studies will be required to obtain a fuller understanding of the variations observed from complex to complex.

The geometry of the Cu(II)–O₂⁻ moiety in 1:1 adducts [(L)Cu(O₂)]⁺ (L = TMPA, TMPAE, BQPA) is not known at present, but we postulate an end-on terminal coordination (Chart 1),^{15,29} similar to that found in the corresponding peroxo complexes, [(L)Cu^{II}]₂(O₂²⁻)²⁺ (**8c**, etc.). Supporting information is the following: (i) Pentacoordination for copper(II) is common and generally preferred, including with these tripodal tetradentate ligands; this leaves only a single binding site (for one oxygen atom of superoxide anion) assuming ligation of all N atoms of the chelate. Note that bidentate side-on μ -peroxo {as well as superoxo coordination in Cu^{II}(O₂⁻)(HB(3-*t*Bu-5-*i*Prpz)₃)} has only been established in systems with tridentate donor ligands.¹ (ii) Spectral characteristics for Cu(II)–O₂⁻ complexes with TMPA and TMPAE ($\lambda_{\text{max}} = 410$ – 416 nm) differ considerably from those seen for Cu^{II}(O₂⁻)(HB(3-*t*Bu-5-*i*Prpz)₃), vide supra. As mentioned, [(BQPA)Cu(O₂)]⁺ has somewhat different UV–vis properties ($\lambda_{\text{max}} = 378$ nm), perhaps perturbed by the quinoyl environment.

Comparison to Fe and Co. The kinetics and thermodynamics of formation of [(L)Cu(O₂)]⁺ species may also

Table 4. Typical Kinetic–Equilibrium Constants for Room-Temperature M:O₂ = 1:1 O₂ Binding

system	k_1 (O ₂) (M ⁻¹ s ⁻¹)	K_1 (M ⁻¹)
hemoglobins/myoglobins	10 ⁷ –10 ⁸	10 ⁵ –10 ⁶
porphyrin–iron models	10 ⁷ –10 ⁸	10 ⁵ –10 ⁶
cobalt complexes	10 ² –10 ⁷	10 ² –10 ⁷
tripod–ligand–Cu ^I complexes	6 × 10 ⁴ –8 × 10 ⁷	0.3–0.4
hemocyanins	10 ⁷ –10 ⁸	10 ⁵ –10 ⁶
cytochrome <i>c</i> oxidase (Cu _B)	3.5 × 10 ⁸	7 × 10 ³

be compared to data available for related iron and cobalt M–O₂ species (Table 4).^{15,26,27,30,31} Comparable end-on (hemoglobin-like) coordination of superoxide anion to M(III) is implicated for O₂ bound to cobalt(II) complexes, heme proteins, or heme model iron(II) complexes. Second-order rate constants for “on” O₂ binding to the tripodal–ligand–copper(I) complexes are as great or greater (6 × 10⁴ to 8 × 10⁷ M⁻¹ s⁻¹, 298 K) than values observed for Fe(II) or Co(II). Thus, k_1 for [(TMPA)Cu^I(RCN)]⁺ (**1a**) compares to that observed for initial reaction with the reduced Fe···Cu binuclear cyt *a*₃–Cu_B active site in cytochrome *c* oxidase (postulated as a transient Cu_B–O₂ species),⁵ as well as for deoxyhemocyanin, where kinetic studies^{24,32} thus far reveal only a single-step O₂ binding process. However, room-temperature equilibrium constants for [(L)Cu(O₂)]⁺ formation in EtCN solvent (Table 1) are orders of magnitude reduced compared to values for Fe or Co. These differences are therefore ascribable to variations in the off-rate k_{-1} ; O₂⁻ is more tightly bound to the higher oxidation state M(III) species. This may be especially significant for the case of Co(III), which is always low-spin (d⁶). Strong M(III)–O₂⁻ bonding is supported by examination of ΔH° values (for M(II) + O₂ ⇌ M(III)–O₂⁻), commonly found in the range $\Delta H^\circ_{\text{formation}} = -40$ to -80 kJ mol⁻¹ for natural or synthetic hemes, cobalt porphyrins, and cobalt complexes,^{15,26,33} compared to the $\Delta H_1^\circ = -32$ to -35 kJ mol⁻¹ range for formation of [(L)Cu^{II}(O₂)⁻]⁺. Compared to our copper complexes, similar or even far more unfavorable negative ΔS° values are found in Fe(II)–O₂ and Co(II)–O₂ reactions, except for certain cases found in nature.²⁴ There, tertiary structure conformational changes in the protein matrix presumably overcome the inherently unfavorable loss of translational entropy of O₂ binding to metals ions.

Cu:O₂ = 2:1 Peroxidocopper(II) Complex Formation.

As mentioned, kinetic Scheme 3 applies to all the tetradentate ligand complexes. In line with the x-ray structure of [(TMPA)Cu^{II}]₂(O₂²⁻)²⁺ (**8c**), the closely matching pattern and intensities of UV–vis bands for Cu:O₂ = 2:1 adducts implicate similar *trans*- μ -1,2-peroxidocopper(II) structures for species formed with TMPA, TMPAE, BPQA, and BQPA (as an “intermediate”), $\lambda_{\text{max}} = 525, 532, 535,$ and 545 nm, respectively. Interestingly, activation enthalpies pertaining to Cu–O bond splitting for the peroxo complexes (k_{-2} , bottom equation in Scheme 3) are all roughly 65 kJ mol⁻¹, which also match the values observed for the related process k_{-1} (top equation in Scheme 3). This finding seems consistent with (i) terminal coordina-

tion and (ii) a {Cu(II)–O–O} description for superoxo-copper(II) and peroxidocopper(II) species alike. Studies on oxygenation of cobalt(II) complexes with macrocyclic ligands also suggests comparable Co–O bond strengths for peroxo- and superoxocobalt(III).³⁴ The overall forward reaction to form the 2:1 adducts is described by $k_{\text{on}} (=k_1k_2/k_{-1})$, exhibiting a negative ΔH° and highly negative activation entropy (Table 3). Due to the former effect, the rate of 2:1 adduct formation decreases with increasing temperature, due to the preequilibrium constant $K_1 = k_1/k_{-1}$ (i.e., Cu(II)–O₂⁻ formation), which significantly decreases with increasing temperature. Whereas thermodynamic stability is hardly affected at all for 1:1 [(L)Cu(O₂)]⁺ species by increasing steric hindrance, quinolyl-for-pyridyl substitution has a remarkable destabilizing effect on the binuclear complex [(L)Cu]₂(O₂)²⁺ (K_2 and β_2 , Table 3), as two bulkier tetradentate moieties are now brought in close proximity by the μ -peroxo ligand.

[(L)Cu]₂(O₂)²⁺ peroxidocopper(II) formation may also be compared to that observed for μ -peroxidocobalt(III) compounds derived from mononuclear precursors, where the molecularity of reaction is analogous.^{26,27,30} For our copper complexes at 298 K, k_{on} ranges from 5–7 × 10⁵ M⁻² s⁻¹. Both smaller and larger values have been observed for various cobalt complexes.^{30,35,36} In terms of equilibrium binding parameters, Co₂O₂ complexes also exhibit large negative ΔS° values, but considerable room-temperature stabilities (log $K_{\text{eq}} \approx 6$ –15) are derived from much more negative $\Delta H^\circ_{\text{formation}}$ values (e.g., -120 to -150 kJ mol⁻¹), ascribable to stronger binding of peroxide by cobalt complexes with its larger 3+ charge.

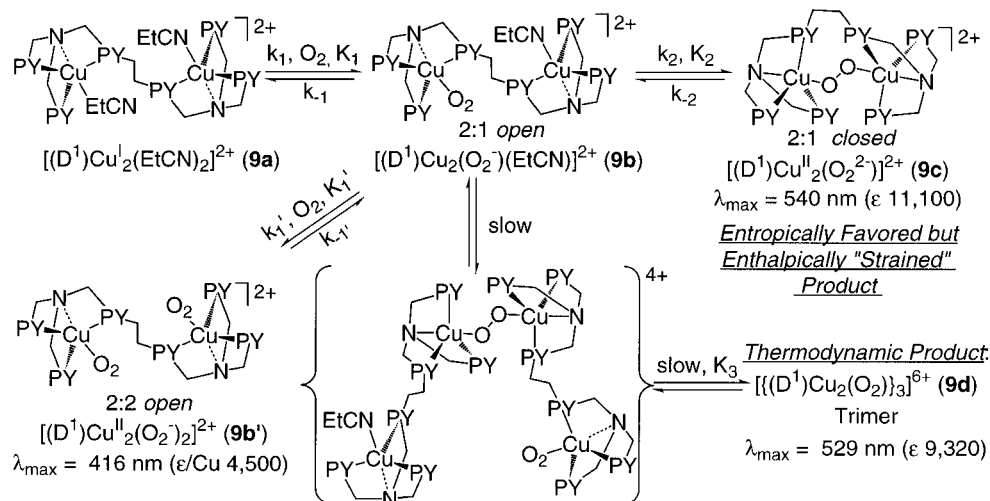
Comparison to a Binuclear Analogue. The ligand D¹ (Chart 2) and resulting binuclear complex [(D¹)Cu₂(EtCN)₂]²⁺ (**9a**) were generated in order to promote intramolecular μ -peroxo formation compared to that in [(TMPA)Cu^{II}]₂(O₂²⁻)²⁺ (**8c**), by overcoming a significant part of the unfavorable reaction entropies observed with TMPA and TMPAE (Table 3). In fact, this expectation was only partly realized.

With D¹, we observe superoxo species with different stoichiometries and statistically related rate constants, according to the two possibilities (**9b** and **9b'**) for Cu:O₂ = 1:1 binding to [(D¹)Cu₂(EtCN)₂]²⁺ (**9a**), Scheme 4.²⁹ Chromophoric characteristics ($\lambda_{\text{max}} = 416$ nm) and kinetic–thermodynamic constants (Table 3) of the mixed-valence 2:1 *open* [(D¹)(Cu^ICu^{II})(O₂⁻)(EtCN)]²⁺ (**9b**) and 2:2 *open* [(D¹)Cu₂(O₂)₂]²⁺ (**9b'**) are quite analogous to those with TMPA and TMPAE.

Formation and Decay of “Strained” μ -Peroxide [(D¹)Cu₂(O₂)]²⁺ (9c**).** The subsequent low-temperature kinetic product is indeed the expected intramolecular μ -peroxo species [(D¹)Cu₂(O₂)]²⁺ (**9c**), Scheme 4. The data in Table 3 reveal that the binucleating nature of D¹ leads to significant entropic stabilization of [(D¹)Cu₂(O₂)]²⁺ (**9c**), in relation to [(TMPA)Cu]₂(O₂)²⁺ (**8c**). Activation entropies associated with **9c** formation (k_2, k_{on}) are 60–70 J K⁻¹

(30) Bakac, A. *Prog. Inorg. Chem.* **1995**, *43*, 267–351.(31) Momenteau, M.; Reed, C. A. *Chem. Rev.* **1994**, *94*, 659–698.(32) Andrew, C. R.; McKillop, K. P.; Sykes, A. G. *Biochim. Biophys. Acta* **1993**, *1162*, 105–114.(33) Rybak-Akimova, E. V.; Masarwa, M.; Marek, K.; Warburton, P. R.; Busch, D. H. *Chem. Commun.* **1996**, 1451–1452.(34) Wong, C.-L.; Switzer, J. A.; Balakrishnan, K. P.; Endicott, J. F. *J. Am. Chem. Soc.* **1980**, *102*, 5511–5518.(35) Donatsch, P.; Gerber, K. H.; Zuberbühler, A.; Fallab, S. *Helv. Chim. Acta* **1970**, *53*, 262–268.(36) Zuberbühler, A.; Kaden, T.; Köchlin, F. *Helv. Chim. Acta* **1971**, *54*, 1502–1508.

Scheme 4



mol⁻¹ more favorable than those for **8c**, while copper–dioxygen bond splitting (k_{-2}) is 70 J K⁻¹ mol⁻¹ entropically disfavored for the binuclear complex. The result is a substantial thermodynamic entropic stabilization by 130–140 J K⁻¹ mol⁻¹ (K_2 and β_2) for this *closed* peroxo form **9c**, in relation to **8c**. Recall the nearly identical equilibrium parameters for superoxo formation with D¹ and TMPA (i.e., K_1 , ΔH_1° , ΔS_1°), which further strongly supports the explanation of entropic stabilization of $[(D^1)Cu_2(O_2)]^{2+}$ (**9c**), via favoring of *intramolecular* μ -peroxo bridge binding. However, favorable entropy terms for **9c** formation are offset by concomitant enthalpic destabilization, both kinetically (ΔH_2^\ddagger , ΔH_{on}^\ddagger) and thermodynamically (ΔH_2° , ΔH_{on}°). The interpretation of this finding is that $[(D^1)Cu_2(O_2)]^{2+}$ (**9c**) possesses a strained structure, characterized by a charge-transfer transition $\lambda_{max} = 540$ nm, shifted from $\lambda_{max} = 525$ nm in $[(TMPA)Cu_2(O_2)]^{2+}$ (**8c**) (but closer to values seen for sterically encumbered and less stable peroxo complexes with BPQA (535 nm) and BQPA (545 nm)). Activation enthalpies related to $[(D^1)Cu_2(O_2)]^{2+}$ (**9c**) are 20 kJ mol⁻¹ higher for dioxygen binding (k_2 , k_{on}), but more than 20 kJ mol⁻¹ lower for Cu–O bond splitting (k_{-2}), as compared to $[(TMPA)Cu_2(O_2)]^{2+}$ (**8c**). The net result is a massive loss in overall enthalpy of formation ΔH_{on}° , reduced to -35 kJ mol⁻¹ for **9c**, compared to -81 kJ mol⁻¹ for **8c**. Ring closure (i.e., peroxo formation) itself (K_2) has a negligible or even slightly endothermic reaction enthalpy, 0.5 kJ mol⁻¹.

In fact, $[(D^1)Cu_2(O_2)]^{2+}$ (**9c**) is not the ultimate oxygenation product of **9a**, and at higher temperatures a rearrangement occurs ($\lambda_{max} \rightarrow 529$ nm). Kinetic analysis²⁹ reveals this product must be a trimer species, $[(D^1)Cu_2(O_2)_3]^{6+}$ (**9d**), having a closed annular structure which provides for relief of steric constraints via formation of intermolecular Cu–O₂–Cu bonds, Scheme 4. For **9d**, formation from **9a** (i.e., $3(9a) + 3O_2 \rightleftharpoons 9d$) yields $K_3 = 3 \times 10^{28} \text{ M}^{-5}$ at 183 K, $\Delta H_3^\circ = -153 \text{ kJ mol}^{-1}$, $\Delta S_3^\circ = -289 \text{ J K}^{-1} \text{ mol}^{-1}$. On a per Cu:O₂ = 2:1 (i.e., peroxo moiety) basis, the enthalpy of formation for **9d** ($\Delta H^\circ = -51 \text{ kJ mol}^{-1}$) lies between those for the peroxodicopper(II) moieties in $[(D^1)Cu_2(O_2)]^{2+}$ (**9c**) (-35 kJ mol^{-1}) and

$[(TMPA)Cu_2(O_2)]^{2+}$ (**8c**) (-81 kJ mol^{-1}). Thus, **9c** is the most strained, and rearrangement affords **9d** for which much but not all of the strain is released relative to that found in the parent system **8c**. Note that the λ_{max} value for the charge-transfer transition in these D¹ and quinolyl ligand species appears to track this relative stability.

The results with D¹ show that a binucleating ligand may indeed favor formation of intramolecular peroxo species, but in this case at least, enthalpic destabilization occurs. The resulting intramolecular strain is released by oligomerization. Thus, rearrangement reactions giving intermolecular μ -peroxo complexes may be a general phenomenon; this process, by definition, cannot occur for oxygenation reactions with mononuclear systems.

Concluding Remarks

Use of appropriate ligands, low-temperature synthesis and handling, and advanced stopped-flow kinetic methods and analysis have provided detailed insights into the kinetics–thermodynamics of formation of several kinds of superoxocopper(II) (Cu–O₂) and peroxodicopper(II) (Cu₂–O₂) complexes. Dioxygen binding is as strong (enthalpically) as for biological O₂ carriers (including hemocyanin),²⁴ but room-temperature stability is precluded by unfavorable entropies for these low-molecular-weight systems. We consistently observed a general trend of compensating favorable enthalpies with less favorable entropies (and vice versa), restricting the range of overall stabilities. It is important to note that in our experience comparisons of kinetic or equilibrium constants at a given temperature can sometimes be very misleading, and we caution that discussion of activation or thermodynamic parameters should be preferred wherever possible.

The tripodal-ligand systems (e.g., TMPA) provide the first insights into consecutive superoxo- and peroxocopper formation, with end-on ligation. Binucleating ligands provide for faster peroxo Cu₂–O₂ formation due to entropic factors; the rate of O₂ binding by deoxyhemocyanin ($\sim 10^7 \text{ M}^{-1} \text{ s}^{-1}$)³² can be achieved even at low temperature, with the phenoxo-bridged complex $[Cu_2(XYL-O^-)]^+$ (**4**). But, as seen with D¹, steric constraints may cause (enthalpic) destabilization in a μ -peroxo species within a

binuclear complex, leading to subsequent rearrangement. While tetradentate ligands favor end-on coordination, tridentate ligands give side-on bridging $\mu\text{-}\eta^2\text{:}\eta^2\text{-peroxo}$ products. With the N4 ligand system, both types of adducts could be observed; an end-on $\mu\text{-}\eta^1\text{:}\eta^1\text{-peroxo}$ intermediate species forms more rapidly, before rearranging to the considerably more enthalpically stable side-on $\mu\text{-}\eta^2\text{:}\eta^2\text{-peroxo}$ product. Given the nature of the protein structures, it is tempting to postulate that a similar process occurs with O₂ binding to deoxyhemocyanin, affording a molecular mechanism which can drive subunit–subunit cooperative interactions.

The systems described show how important insights can be obtained by varying ligand electronic and steric factors, and still further systematic investigations are needed to explain observations of a subtle nature, as well as to answer major questions. How do rates and stability of copper–dioxygen complexes vary with Cu^{II}/Cu^I redox potentials? How do solvent–environmental factors influence O₂ binding kinetics, thermodynamics, or even preferred structure? Which kind of structure directly or

- (37) Recent measurements reveal that room-temperature stability of a Cu₂O₂ species can be obtained with D¹ or a modified ligand, in acetone as solvent. Karlin, K. D.; Lee, D.-H.; Kaderli, S.; Zuberbühler, A. D. *Chem. Commun.* **1997**, in press.
- (38) El-Sayed, M.; Ismail, K. Z.; El-Zayat, T. A.; Davies, G. *Inorg. Chim. Acta* **1994**, *217*, 109–119.
- (39) Becker, M.; Schindler, S.; van Eldik, R. *Inorg. Chem.* **1994**, *33*, 5370–5371.
- (40) Projahn, H.-D.; Schindler, S.; van Eldik, R.; Fortier, D. G.; Andrew, C. R.; Sykes, A. G. *Inorg. Chem.* **1995**, *34*, 5935–5941.
- (41) Goldstein, S.; Czapski, G.; van Eldik, R.; Cohen, H.; Meyerstein, D. *J. Phys. Chem.* **1991**, *95*, 1282–1285.

eventually leads to reactive (electrophilic or nucleophilic) oxygenating species? How can room-temperature stability be achieved in a synthetic system?³⁷ Can D¹ be easily modified to eliminate strain, or are highly preorganized systems required? Kinetic studies involving formation of copper–dioxygen adducts is also being pursued by other research groups.^{20,38–41} A point regarding the aforementioned²⁵ triazacyclononane ligand LCu(I)–O₂ chemistry is of interest; in contrast to our tripodal systems, formation of the superoxo–Cu(II) species appears to be rate limiting.²⁰ Tolman's findings^{20,25} concerning equilibrium formation of $\mu\text{-}\eta^2\text{:}\eta^2\text{-peroxodicopper(II)}$ and isomeric bis($\mu\text{-oxo}$)dicopper(III) species beg the question, can or do [Cu₂(R-XYL-H)(O₂)]²⁺ (**2**) or [Cu₂(N4)(O₂)]²⁺ (**10**) (or its relatives)¹⁶ undergo a similar process, and is the side-on peroxo or bis($\mu\text{-oxo}$)dicopper(III) isomer of **2** the reacting species in the xylyl hydroxylation? While much work remains in elucidation of fundamental aspects of copper–dioxygen adduct formation, future directions also include matters pertinent to O–O bond cleavage, i.e., with accompanying reduction–protonation and/or substrate oxygenation chemistry, relevant to biological O₂ processing and catalysis.

We are very appreciative of the efforts of our graduate students and postdoctorals, whose names appear in the references. We also thank the National Institutes of Health (K.D.K.) and Swiss National Science Foundation (A.D.Z.) for financial support of this research.

AR950257F